https://doi.org/10.20965/jdr.2019.p0416

Paper:

Development and Validation of a Tsunami Numerical Model with the Polygonally Nested Grid System and its MPI-Parallelization for Real-Time Tsunami Inundation Forecast on a Regional Scale

Takuya Inoue[*1,*2,†], **Takashi Abe**[*1], **Shunichi Koshimura**[*1], **Akihiro Musa**[*3,*4], **Yoichi Murashima**[*1,*5], **and Hiroaki Kobayashi**[*6]

[*1]International Research Institute of Disaster Science, Tohoku University
468-1 Aramaki Aza Aoba, Aoba-ku, Sendai, Miyagi 980-0845, Japan
[†]Corresponding author, E-mail: takuya_inoue@kk-grp.jp
[*2]Kokusai Kogyo Co., Ltd., Tokyo, Japan
[*3]Cyberscience Center, Tohoku University, Miyagi, Japan
[*4]NEC Corporation, Tokyo, Japan
[*5]RTi-cast Inc., Miyagi, Japan
[*6]Graduate School of Information Sciences, Tohoku University, Miyagi, Japan
[Received October 31, 2018; accepted February 19, 2019]

We have developed a new numerical model suitable for rapid and wide-area estimation of tsunami inundation and damage. The model is based on the world-renowned TUNAMI code solving the two-dimensional nonlinear shallow water equations, and enables one-stop simulation of the initial tsunami distribution based on a fault model, tsunami propagation and inundation, and damage estimation. It extends the configuration of the grid system from conventional rectangular regions to polygonal regions so that deployment of high-resolution grids can be confined to the coastal lowland, resulting in remarkably improved efficiency in computation and better precision. For the purpose of real-time implementation of tsunami inundation simulation using a high-performance computing infrastructure, vectorization and MPI parallelization have also been conducted. Moreover, the model was verified and validated through several benchmark problems that the National Tsunami Hazard Mitigation Program, organized by federal agencies and states in the U.S., developed as the quality standards for simulating and assessing tsunami hazard and risk. The newly-developed model is named "Real-time Tsunami inundation (RTi) model," and its computational performance was examined using the SX-ACE, a vector supercomputer installed at Tohoku University. The results show that it requires only 128 cores of the SX-ACE for implementing six-hour tsunami inundation simulation with a 10-meter grid resolution within 10 minutes for the 700 km long coastline of Kochi Prefecture, Japan. This means that the RTi model is over 10 times more efficient as the conventional tsunami model with the rectangular domains, and it can be inferred that 2,451 cores of the SX-ACE are the overall computational resources needed for real-time tsunami inundation forecast on the whole coastal regions along the Nankai Trough subduction zone, corresponding to the computational performance of 170 Tflop/s. The resources required are equivalent to 24% of all the SX-ACE resources at Tohoku University, indicating the feasibility of real-time tsunami inundation forecast on a regional scale by using the RTi model. Since the Disaster Information System operated by the Cabinet Office of the Japanese Government adopted a function of tsunami damage estimation using the aforementioned numerical model, at the end of this paper, a brief overview of the subsystem for rapidly estimating tsunami damage on a regional scale is described.

Keywords: tsunami, real-time simulation, inundation forecast, high-performance computing, verification and validation

1. Introduction

Experience of the disaster of the 2011 Great East Japan Earthquake and Tsunami taught us that an unanticipated huge disaster is possible. It is recognized that it takes a considerably long time to grasp the whole picture of damage in a catastrophic natural disaster like the 2011 event. It is said that municipal officials at the city of Ishinomaki in Miyagi Prefecture in Japan devoted 14% of their working hours to information gathering during the first 5 days after the earthquake occurrence [1]. Without having an appropriate overview of damage, it is difficult to carry out proper disaster responses. However, aerial surveys and/or field surveys cannot be conducted during the nighttime, and there is also a risk of secondary disaster in information collection immediately after the occurrence of a natural disaster. If it is possible to rapidly and automatically estimate damage situations using ever-improving

ICT, therefore, we are able to make disaster countermeasures more efficient and effective, leading to considerable social benefits.

In this paper, such an ICT technology, the real-time estimation of tsunami inundation and damage, is discussed. We narrow an argument down to near-field tsunamis, which arrive at the coastline in a shorter time period compared to far-field tsunamis and demand higher technology in terms of time constraint. Here we define the keyword "real-time" as the time scale in which tsunami waves arrive at the coast after earthquake occurrence. It is then assumed that 10 minutes are given for evaluation of tsunami inundation and its damage. The forecast period is set to 6 hours in order not to underestimate an overall picture of tsunami inundation areas. Forecasting 6-hour situations in the future within 10 minutes is indeed "much faster than real-time." However, it should be reasonable to set the target of 10 minutes because some coastal regions are said to be affected by tsunamis in quite a short time, and because it also takes substantial time both for high-precision estimation of initial conditions like fault models and for the dissemination of information to disaster responders. It goes without saying that disaster response will start sufficiently earlier than 6 hours after an earthquake occurs.

The accuracy of tsunami inundation simulation depends on the extent to which a numerical model is able to represent tsunami inundation behaviors on land. Therefore, the approximate accuracy of bathymetry/topography data is of much importance [2]. It is recommended in the technical guide for assessment of tsunami inundation issued by the Japanese authorities that spatial resolution of about 10 meters or finer should be used [3]. Generally speaking, the two-dimensional nonlinear shallow water equations (NSWEs) are used in tsunami simulation for a spatial extent as large as a city area because the complete set of Navier-Stokes equations or any kind of their three-dimensional approximations is computationally infeasible at the present time. With a grid resolution as fine as 10 meters, however, NSWEs are computationally expensive enough. It could take a couple of days on an ordinary workstation to implement 6-hour time integration, meaning that computational loads are the apparent bottleneck in real-time tsunami inundation modeling.

A simple solution to the problem of the computational cost is a precomputed database storing scenarios of tsunami source models and consequent inundation situations so that a more plausible scenario is extracted on the basis of observations immediately after earthquake occurrence. Among these database-driven approaches, Takahashi et al. [4] adopt the DONET ocean-bottom pressure gauges in the Nankai Trough region, and their forecast system has already been in operation in organizations such as Wakayama Prefecture and Mie Prefecture. Yamamoto et al. [5] suggest the same kind of database approach, using the S-net ocean-bottom pressure gauges around the Japan Trench, though their discussion is focused on a method of extracting plausible earthquake scenarios using multiple indices. Gusman et al. [6] devise a method to combine real-time simulation with a coarse grid resolution and pre-computed database of tsunami waveforms and inundation, enabling us to obtain the site-specific best scenario by comparing tsunami waveforms at nearshore points.

The accuracy of a database-driven method is highly dependent on the coverage and contents of the pre-computed scenarios since an unanticipated scenario cannot be chosen. As a matter of course, we are forced to increase the number of scenarios as much as possible, but we then encounter the challenge of computational loads due to the non-negligible computational cost for inundation simulation of each scenario. For example, Takahashi et al. [4] prepare inundation scenarios for 1,506 fault models, which are a subset of fault models set by Baba et al. [7]. They assume an earthquake fault has a uniform slip and omit a possible heterogeneous slip distribution on a fault plane as an approximation. In simulating inundation behaviors of tsunamis, a tidal condition also affects the result significantly, especially for tsunamis with relatively smaller amplitudes. Following a database approach, however, it seems too difficult to deal with varied levels of the tide, considering that this increases the number of scenarios in the database on a multiplication basis. The update of the inundation database is very onerous because coastal protection facilities like seawalls are being improved and land use is being changed year after year in some regions in the world. The Pacific coast of Japan is a good example because there is said to be an imminent risk of a huge earthquake in the Nankai Trough subduction zone and lots of reconstruction work has been executed in Tohoku since the 2011 earthquake and tsunami.

On the contrary, a "forward simulation" approach enables us to circumvent the above-mentioned challenges. This approach simulates tsunami propagation and inundation after earthquake occurrence by incorporating actual sensing data such as estimated earthquake faults and site-specific tidal conditions when tsunami waves arrive at the coast. This reduces the number of possible scenarios drastically, and in turn allows us to utilize more complex and realistic conditions. Taking a tsunami source model, for instance, it becomes possible to adopt slip distribution on a fault plane (for example, [8]), and/or initial sea surface distribution obtained by inversion methods based on offshore tsunami measurements (for example, [9, 10]). We are also free from the challenge of continuously updating the database as far as the latest bathymetry/topography data for forward simulation are maintained.

Owing to the recent advances in high-performance computing infrastructures (HPCI), the fundamental bottleneck of the forward simulation approach, i.e., the computational load, is in the process of being resolved in terms of real-time inundation simulation at least for a spatial extent as large as a city area. Oishi et al. [11] investigate the fastest possible speed of tsunami simulation on a modern parallel computer, and clarified that it takes no more than 93.2 seconds for tsunami inundation simulation in Sendai City with grids as fine as 5-meter resolution when they use 13,498 cores of the K computer, Japan's flagship supercomputer operated by RIKEN. Since they

set the computational period at 2 hours, the computational time is equivalent to about 5 minutes for the six-hour time integration. Musa et al. [12, 13], on the other hand, aim to complete the computation within 10 minutes and demonstrate that real-time tsunami simulations in Kochi City, Shizuoka City, a coastal area including Ishinomaki City and Higashimatsushima City are feasible if they employ for each area 256 cores of the SX-ACE, a vector supercomputer installed at Tohoku University. They also give an overview of the real-time tsunami inundation forecast system in operation for the three target areas. Koshimura, a member of their research team points out that the "10-10-10 (triple ten) challenge" has been achieved, where a tsunami source model is determined within 10 minutes after an earthquake occurs and tsunami inundation simulation and damage estimation with a high-resolution of 10-meter grids is completed within 10 minutes [14].

As reviewed above, the technology of real-time forward simulation regarding tsunami inundation is well known within the tsunami academic and practical community. As is obvious in the 2011 Tohoku tsunami, however, a massive tsunami will devastate not only a city but also a series of coastal areas. Therefore, tsunami inundation forecast on a regional scale is required for effectively assisting disaster responders and inhabitants in coastal lowlands at risk of tsunami. Here we define "regional scale" as coastlines of hundreds to thousands of kilometers. Inoue et al. [15] give a rough estimate of requisite computational resources to conduct real-time tsunami simulation with a 10-meter resolution in the entire Nankai Trough region through actual numerical simulations of 390 calculation regions used in the damage estimation carried out by Japanese Government [16], and the results show that 29,408 cores of the SX-ACE are needed, which is about three times more than all the SX-ACE resources at Tohoku University. This denotes that real-time simulation on a regional scale is virtually impossible by means of the existing numerical model and the HPCI. Therefore, the challenge addressed in this paper is the development of a new model with improved efficiency in terms of wide-area simulation of tsunami inundation.

An effort to apply numerical simulation to activities of disaster prevention and mitigation could be ineffectual, or even result in harm, if the numerical method does not return accurate results. In that case, the development of HPCI or a computationally inexpensive model would have no value. Referring to Babuska and Oden [17], the validation of a numerical model is conducted in the following two steps. Firstly, in the verification step, a computational model, obtained by discretizing a mathematical model, is examined in terms of whether it can simulate with sufficient accuracy the mathematical model that is supposed to represent a physical event of concern. Secondly, in the validation step, it is determined whether the mathematical model represents the actual physical event with sufficient accuracy, meaning that the overall numerical model represents the physical phenomenon.

Among the tsunami community in the U.S., the aforementioned process of verification and validation (V&V) is standard practice. A standard, OAR PMEL-135, provides benchmark problems and criteria that tsunami models must meet [18]. Several workshops have been held in order to cross-compare existing models (for example, [19, 20]). Moreover, the National Tsunami Hazard Mitigation Program (NTHMP), organized by federal agencies and states in the U.S., requires that all operational models for tsunami inundation mapping should be properly validated based on the existing standard so that the reliability of inundation maps and a basic level of consistency among parallel efforts to develop tsunami models are ensured [21].

In the practice of tsunami inundation mapping in Japan, validation of a tsunami numerical model is in principle assured by adjusting a tsunami source model for each target area so that reproducibility against field survey data becomes acceptable, according to the technical guide [3]. This process considers uncertainties regarding tsunami source models and bathymetry/topography data. Since we never know the emerging inundation zones or depth in the process of real-time forecasting, validation of a tsunami model must be conducted separately as a numerical model. This reliable procedure of validation allows greater social confidence and acceptance of the real-time inundation forecast due to increasing accuracy in the determination of a tsunami source model and construction of high-precision bathymetry/topography data due to the modern sensing technologies. In this context, V&V of the new model is dealt with as an additional challenge.

There are thus three objectives in this paper. Firstly, we aim to discuss the development of a new tsunami inundation model that is computationally efficient even for a challenging case where wide-areas should be evaluated. Thereby, the configuration of computational grids is extended from conventional rectangular regions to polygonal regions so that deployment of high-resolution grids can be confined to the coastal lowland. This new approach is introduced in the previous works of the authors in the Japanese language [15, 22]. The application of the new model, both for a vector supercomputer system and a system composed of workstations with the many-core architecture, is also discussed in our previous work [23], focusing on the comparison of the computational performance of the two computer systems. This paper focuses more on the perspective of geophysical sciences, and describes the details of the newly-developed grid system, as well as enhanced functions for a one-stop simulation of tsunami propagation, inundation, and damage. It was discovered in the previous work [22] that the new model could have low efficiency when a small number of CPU cores are deployed. This paper also solves this problem, which is a critical issue in practical situations because a massively-parallel computation is not always required. Secondly, we aim to introduce a brief overview of the validation of the newly-developed model by way of the commonly-used benchmark problems organized by NTHMP. Finally, we examine the computational performance of the newly-developed and validated model, and elucidate the feasibility of tsunami inundation simulation with a 10-meter grid

resolution within 10 minutes on a regional scale.

This paper is organized as follows. Section 2 describes the details of the new model for tsunami inundation forecast on a regional scale. Section 3 gives an overview of V&V. In Section 4, the computational efficiency of the model is evaluated, and case studies of real-time tsunami simulation for the entire Nankai Trough region are discussed. We conclude in Section 5 with a brief summary and future prospects.

2. Development of a Tsunami Numerical Model with the Polygonally Nested Grid System and its MPI-Parallelization

2.1. Nonlinear Shallow Water Equations

As a mathematical model, we adopt the two-dimensional depth-integrated nonlinear shallow water equations (NSWEs). This is because our aim is to rapidly forecast an overview of tsunami inundation for a broad area, which does not necessarily require a three-dimensional formulation or weakly-dispersive formulation like the Boussinesq-type equations.

Although mathematical expressions of NSWEs had appeared in the literature already in the late 19th century [24], we make reference to the work of Goto and Shuto in 1980s [25], because they discuss the application of NSWEs to a two-dimensional computation of tsunami run-up. By omitting dispersion terms from their expression, the governing equations are written as

$$\frac{\partial \eta}{\partial t} + \frac{\partial M}{\partial x} + \frac{\partial N}{\partial y} = 0, \quad \ldots \quad (1)$$

$$\frac{\partial M}{\partial t} + \frac{\partial}{\partial x}\left(\frac{M^2}{D}\right) + \frac{\partial}{\partial y}\left(\frac{MN}{D}\right) + gD\frac{\partial \eta}{\partial x} + \frac{gn^2}{D^{\frac{7}{3}}}M\sqrt{M^2+N^2} = 0, \quad \ldots \quad (2)$$

$$\frac{\partial N}{\partial t} + \frac{\partial}{\partial x}\left(\frac{MN}{D}\right) + \frac{\partial}{\partial y}\left(\frac{N^2}{D}\right) + gD\frac{\partial \eta}{\partial y} + \frac{gn^2}{D^{\frac{7}{3}}}N\sqrt{M^2+N^2} = 0, \quad \ldots \quad (3)$$

where η denotes the variation of water surface from the still water level h, and D is the total water depth, i.e., $D = h + \eta$. All variables regarding length are based on the meter. M and N are depth-integrated discharge fluxes per unit length in the unit of m^2/s in x- and y-directions, respectively. The gravitational acceleration, g is set at 9.8 m/s^2. The bottom friction term, which accounts for energy dissipation in NSWEs, is approximated by the common Manning's law. n thus represents the Manning's roughness coefficient ($m^{-1/3}s$).

2.2. TUNAMI-N2 Model

As a computational model, we follow the numerical method and discretization scheme of the TUNAMI (Tohoku University Numerical Analysis Model for Investigation of tsunamis) code, which is widely known and approved by the United Nations Educational, Scientific and Cultural Organization (UNESCO) [26]. The TUNAMI code is based on the finite difference method (FDM) of Eqs. (1)–(3), the flux-conservative mathematical formulations, and adopts staggered grids in space and a leap-frog scheme in time. More specifically in the TUNAMI code, spatial grids have a two-dimensional square lattice structure, and the water level is calculated on a grid center and discharge fluxes on grid edges, facilitating the setting of boundary conditions. The leap-frog scheme, where water level and fluxes are calculated in turns, provides a 2nd order precision in time. The "N2" version of TUNAMI deals with near-field tsunamis including run-up phenomena, and they employ a moving boundary condition for simulating run-up fronts. Moreover, characteristics of the model in terms of numerical precision have been extensively discussed in the literature [25, 27, 28].

It is of pivotal importance in tsunami inundation simulation to stably connect computational domains of finer resolution and those of coarser resolution. This is because a tsunami phenomenon has a spatial scale of hundreds of kilometers offshore and sometimes a scale of meters or even smaller in nearshore waters or onshore, which makes it impractical to compute with a single spatial resolution. This connection of domains is generally called a "nesting" algorithm. Considering the multi-scale nature of tsunamis, an alternative proposition would be to select a discretization scheme with unstructured grids or an adaptive mesh refinement (AMR) algorithm, where grid resolution is refined according to the scale of tsunami behavior. However, we maintain the static FDM framework with square structured grids. This is because in real-time forecasting it is also important to reduce the time required for the processing of mapping results onto a GIS-based visualization system, and to comprehend an estimate of computational time in advance.

The TUNAMI-N2 model adopts a nesting both in time and space directions. Here only the spatial nesting is considered because the temporal nesting requires not only interpolations but also extrapolations for water fluxes on the boundary, which could affect the stability of computation. **Fig. 1** shows the schematics of the nesting. The ratio of spatial resolutions is generally set to 1 : 3. It should be noted that the positive directions of axes are different in the original work [26]. As shown in **Fig. 1(a)** in a one-dimensional case, water levels in the finer region are averaged and given to the grid point of the corresponding position in the coarser region. Conversely, water flux in the orthogonal direction alone in the coarser region is substituted to the corresponding edge position in the finer region. Since the grid system is based on the staggered scheme, an extra cell is introduced on the left side of the finer region to hold the left-most flux value. **Fig. 1(b)**

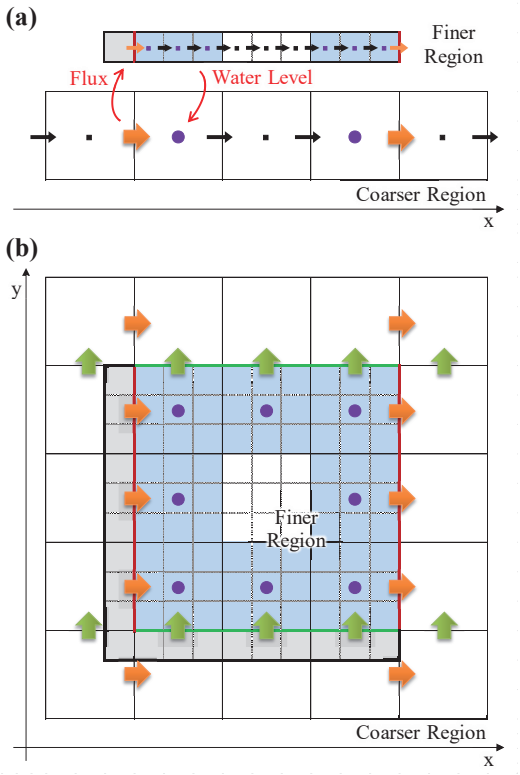

Fig. 1. Schematics of spatial nesting in the TUNAMI code. The panel (a) is a one-dimensional case. Dots and disks are positions for calculation of water levels and arrows are positions for flux calculation. Colored symbols are values used in the nesting operation. Grids filled with light blue are finer cells used for averaging. Bold colored lines in the finer region are positions for interpolation of fluxes, and a gray grid is an extra cell to hold flux values on domain edges. A two-dimensional case is shown in the panel (b), only with symbols relevant to nesting in the coarser region for better visibility.

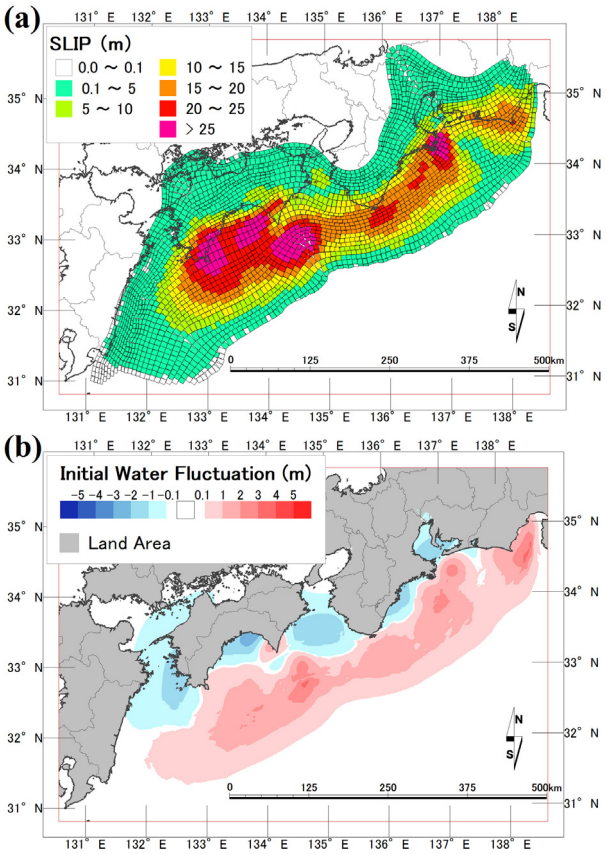

Fig. 2. Examples of a fault model consisting of many fault elements (a), and initial water fluctuations (b). This fault model is about the 1707 Hoei Earthquake and has 2,951 sub-faults. Inoue et al. [30] describe the details of a method to approximately represent slip distribution on a fault plane by a set of rectangular sub-faults.

introduces a simple extension to a two-dimensional case. Water flux in the finer region is now given by interpolating adjacent two values in the coarser region. There are lines of extra cells on the left- and bottom side of the finer region.

2.3. Enhancement of Functions for Real-time Evaluation of Tsunami Inundation and Damage

For the purpose of the real-time forecast of tsunami inundation and damage, we have equipped additional functions within the original TUNAMI code. There are two essential challenges. One is a one-stop computation of tsunami damage from a source model like an earthquake fault model. The other is speed. The following additional functions are solutions mainly to the first challenge:

i. *Estimation of crustal deformation:* Based on a fault model given immediately after earthquake occurrence, crustal deformation is estimated by Okada's method [29]. Through bilinear interpolation, estimated deformation values for a domain with coarse resolution, e.g., 810 m, are given to domains with finer grids, which results in reduced computational loads in calculating deformation and the increased number of fault elements feasible to process in real-time (**Fig. 2(a)**).

ii. *Consideration of the effect of horizontal and short-wavelength displacement:* The effect of horizontal displacement and sea-bottom slope in tsunami generation, whose importance was indicated by Tanioka and Satake [31], is taken into consideration. This could introduce components with highly short-wavelength in deformation, and thus Kajiura's method [32] is applied in order to obtain appropriate initial water fluctuations as an initial condition for tsunami propagation (**Fig. 2(b)**).

iii. *Initiation by initial water fluctuations data:* High-precision tsunami source models based on offshore tsunami measurements (for example, [9, 10]) are available, and tsunami simulation can be initiated through the use of data on water surface fluctuations as well.

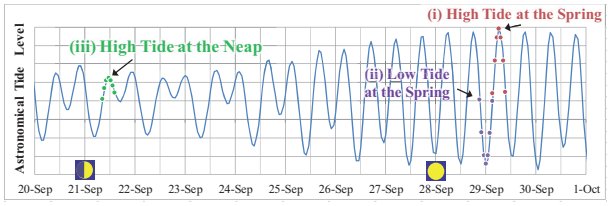

Fig. 3. Schematics of estimation and setting of astronomical tide. Tide levels (filled disks) are estimated at hourly intervals during the forecast period, 6 hours in this case. The maximum value of them is adopted as a tidal condition (black arrow). This function provides a tsunami inundation model with a weekly trend in tide levels such as a spring or a neap, and a trend in the order of hours such as high or low, which is shown in the three cases (i) to (iii) in the figure.

iv. *Estimation of astronomical tide:* Based on the occurrence time of an earthquake, astronomical tide for a target site is computed using harmonic analysis, and the maximum tidal level during the forecast period is adopted as a realistic tidal condition (**Fig. 3**).

v. *Dry grids at the beginning:* Dry areas, regardless of a tidal condition when an earthquake occurs, can be designated for appropriately evaluating inundation information in a below-sea-level area.

vi. *Damage estimation:* Utilizing the simulation result of the distribution of inundation depth, damage estimation based on a fragility curve is seamlessly conducted [33]. A tsunami fragility curve represents the probability of exceedance of certain damage as a function of a quantity related to a tsunami hazard such as inundation depth, which enables statistical and quantitative estimation of tsunami damage on land.

vii. *Hourly output of various data:* Various output data can be obtained at hourly intervals, including maximum inundation depth and start time of inundation. For the details of outputs, Musa et al. [13] can be referred to. All input/output data in the form of two-dimensional distribution are handled as binary data in order to minimize the overall execution time.

viii. *Arbitrary computational domains regarding number, resolution, extent:* Arbitrary domains regarding domain numbers, resolution, and extent can be used by giving conditions including time step specific to bathymetry near a target site in an external file. This facilitates operation and maintenance of the tsunami model as a subsystem of a tsunami forecast system.

2.4. Extension to the Polygonally Nested Grid System

The new model addresses the second challenge, i.e., computational speed, by extending the configuration of computational domains from conventional rectangles to polygons [15].

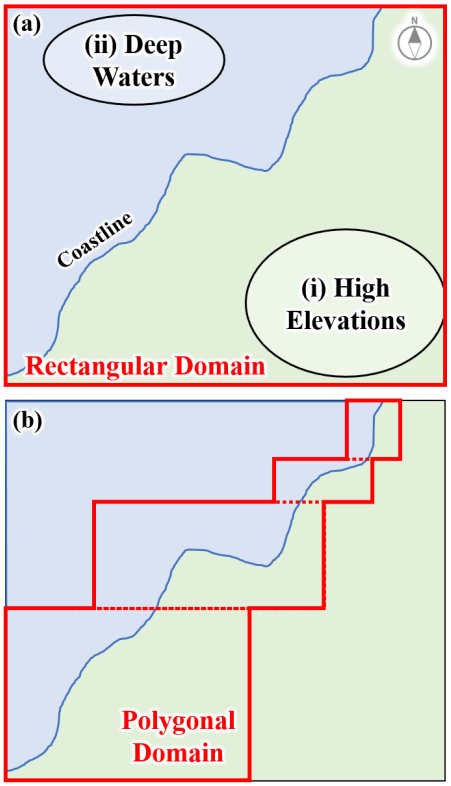

Fig. 4. Schematics of the two obstacles in a wide-area simulation (a) and extension to the polygonal domain (b). Solid lines in red designate borders of computational domain, and dashed lines are borders of polygonal blocks.

As shown in **Fig. 4(a)**, tsunami inundation simulation with the conventional rectangular domain will obviously face two obstacles in covering wider areas. Firstly, a computational domain includes high elevations that will not be inundated but increase the load on operation and memory. Secondly, deep waters are also included in the domain. This is more severe because the larger depth in bathymetry leads to a more stringent CFL condition, considering the CFL condition, in this case, is given as

$$\Delta t \leq \frac{\Delta x}{\sqrt{2gh_{\max}}}, \quad \cdots\cdots\cdots\cdots\cdots (4)$$

where Δt is a time step in integration, Δx is spatial resolution, and $h_{\max}$ denotes the maximum water depth in the computational domain. When it comes to regional estimation as large as coastlines of several hundred kilometers, Δt is forced to become minimum, which results in division of coastlines into many small regions and repetition of evaluation for each of them as shown in **Fig. 5(a)**. There are futile costs in computing duplicate offshore domains of coarser grid resolutions. Overlapped areas between adjacent coastal domains of the finest resolution are also cumbersome especially for coastal plains where a computational domain should be made sufficiently large in order to avoid deterioration of computational precision. This is due to refection of a tsunami flow from an edge of a domain on land.

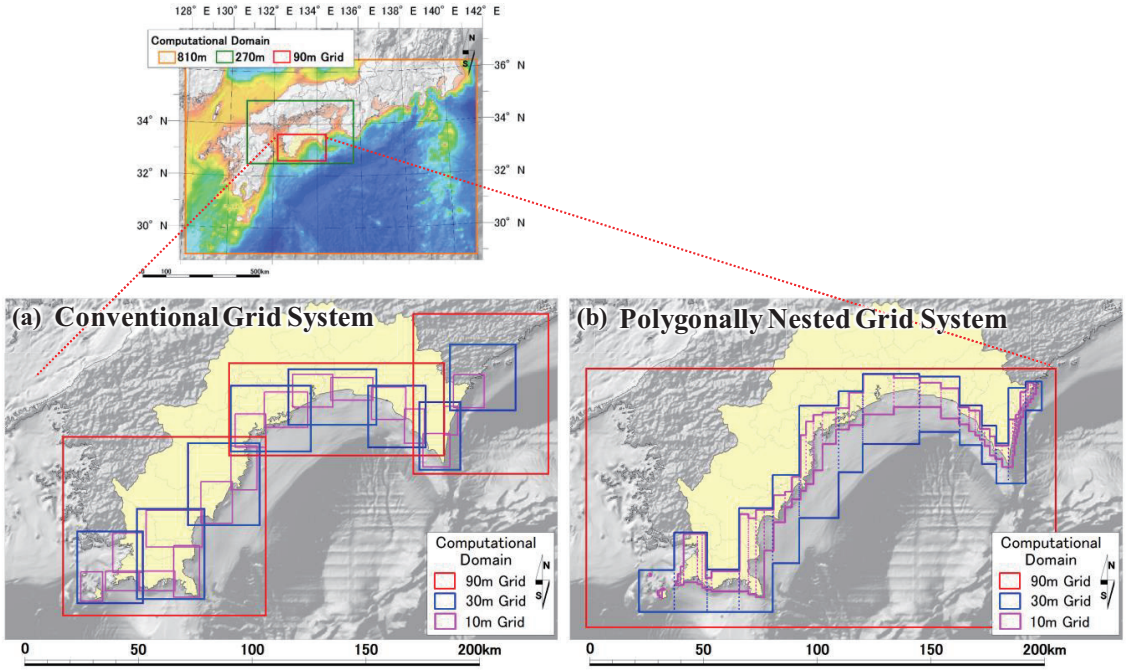

Fig. 5. Examples of grid systems for wide-area tsunami simulation regarding Kochi Prefecture in Japan, together with configurations of offshore domains with coarser grids. The panel (a) gives an example of a grid system with conventional rectangular domains. It is used in the damage estimation carried out by Japanese Government [16]. The system consists of 17 regions in order to cover the prefecture. The prefectural land is colored yellow. The polygonally nested grid system is shown in the panel (b). Dashed lines denote borders of polygonal blocks. The number of polygonal blocks is 14 for the domain of 30-meter resolution, and 49 for 10-meter resolution, respectively. The number of grid points in all 5 domains amounts to about. 35 million, and the time step is 0.2 second. Both systems are defined in the Rectangular Plane IV coordinates, Japanese Geodetic Datum 2000.

A polygonal domain, which is shown in **Fig. 4(b)**, can overcome these obstacles. The new computational domain deploys high-resolution grids only in the coastal lowland. A series of coastlines are situated within a domain, leading to better precision in terms of reflection of a tsunami flow from a domain edge. Deep waters are simulated with a coarser Δx, ameliorating the requirement for Δt. A polygon is constructed by stacking one rectangular "block" from another northward, which in principle corresponds to the direction of the outer loop of the FDM scheme. That is, a tsunami numerical model with the polygonal domain can be regarded as an improved version of the parallel tsunami model with the one-dimensional uneven domain decomposition method. An extent of calculation in the inner-loop direction (i.e., east-west direction in the case of **Fig. 4**) is just contracted by designating proper starting/finishing positions for each polygonal block.

Fig. 5(b) exhibits a polygonally nested grid system, taking an example of Kochi Prefecture whose coastline length reaches about 700 km. Generally speaking, it is better to stack polygonal blocks in the along-coast direction so that an extent of calculation perpendicular to the coastline can be easily adjusted according to depth counters. As is shown in **Fig. 5**, the coastline of Kochi Prefecture extends in the east-west direction, and deep waters are surrounded by land. That is why it is difficult to construct a polygonal system by aligning blocks northward, and the transposition function of the north-south and east-west directions has been implemented. In a transposed system like that for the Kochi Prefecture in **Fig. 5(b)**, the outer-loop direction in the FDM scheme points to the East and the inner-loop direction to the North, respectively.

The new model with the polygonal system is also very effective when target sites are scattered, as in the case of islands (**Fig. 6**). Using the conventional grid system, a number of disjointed regions are required to cover all the targets. The new model, however, is not able to compose torus-shape grids since blocks are aligned in one direction.

An extended nesting scheme is explained in **Fig. 7**. Due to the straightforward nesting method of the TUNAMI code shown in **Fig. 1(b)**, water levels and discharge fluxes orthogonal to the boundary are simply exchanged between coarser and finer regions, along the more complex boundary lines of domains in the case of the polygonal grid system. Compared to the rectangular grid system, there are more corners of the finer region and angles, corresponding to corners for the coarser region in the nesting. These corners and angles might cause instability in computation when the direction of tsunami propagation is oblique to the domain edges. Using a verification calculation in various bathymetric/topographic conditions with multiple spatial resolutions, this nesting scheme for the polygonally nested grid system has proven to be sufficiently stable [15, 22].

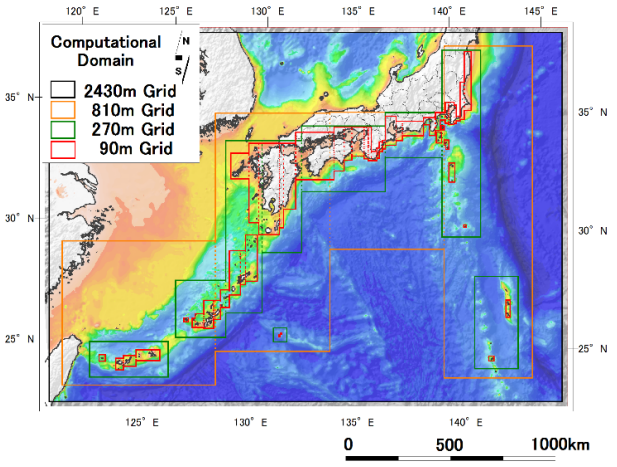

Fig. 6. Configuration of a polygonally grid system for the entire Nanaki Trough region at the resolution of 90 meters. The number of polygonal blocks is 4 for the domain of 810-meter resolution 9 for 270-meter resolution, and 52 for 90-meter resolution, respectively. The total number of grid points is about 49 million, and the time step is 0.5 second. It is defined in the UTM 53 coordinates, WGS 84.

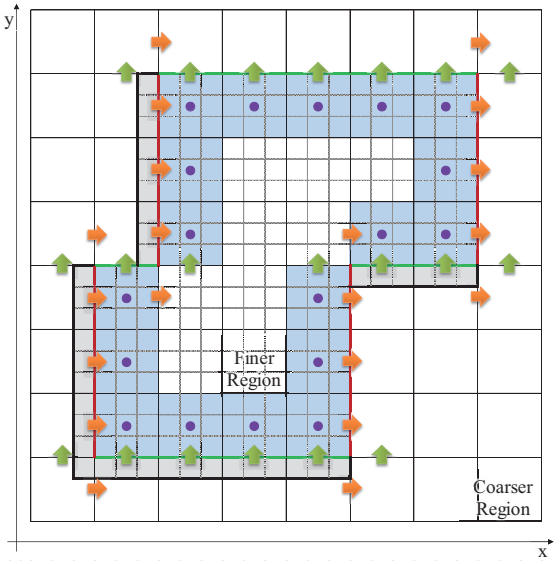

Fig. 7. Schematics of spatial nesting in the new model with polygonally nested grid system. In like manner in **Fig. 1(b)**, only symbols relevant to nesting in the coarser region are shown. Purple disks are positions for interpolation of water levels. Grids filled with light blue are finer cells used for averaging water levels. Arrows are positions for flux calculation, which in turn are interpolated and given to the position of bold and colored lines in the finer region. Gray grids in the finer region are extra cells to hold flux values on domain edges.

2.5. Vectorization and MPI-Parallelization

As computing environment, we mainly discuss the SX-ACE system, which is a system based on a vector supercomputer. Owing to "vector operation," in which calculation for multiple grid points are conducted at one time, and high memory bandwidth, SX-ACE is able to exhibit outstandingly high computational performance compared to an ordinary system with the scalar architecture in the specific problem of the two-dimensional explicit FDM for tsunami simulation [12, 13]. The number of grid points simultaneously processed, which is called the "vector length," is 256 for the SX-ACE.

In vector operations, a "mask operation" is adopted, where both cases are first computed at a conditional branch (if-statement) and then results of only the true case are taken. This indicates that complex conditional branches in time integration lead to decreased computational efficiency. The upwind scheme employed for advection terms in the momentum equation is an easily comprehensive example, and we have optimized the code as is shown in **Fig. 8**. The maximum number of layers of conditional branches in the momentum equation has been trimmed from 5 to 3. Moreover, the original code for the momentum equation determines whether resultant water flux is supposed to be zero two times. Firstly, it is a case where a grid edge is at a sufficiently high elevation such as 50 meters above the calculation datum. Secondly, both of the adjacent grids are dry or water level of a wet grid is lower than the elevation of a dry grid in calculating stricter condition and the first condition can be omitted. Although here we discuss the implementation of the new model on a vector supercomputer, improved efficiency is also expected on a scalar computer through the above-mentioned optimization. Code optimization has been conducted by confirming that computational efficiency on an ordinary workstation does not deteriorate, as well as for other more trivial modifications that do not change the structure of the original code.

Regarding parallelization, the MPI protocol with one-dimensional uneven decomposition of computational domains is adopted. More specifically for the model with the polygonal grid system, each polygonal block is computed by an MPI process when a single CPU core is allocated or decomposed along the outer loop of the FDM scheme when multiple cores are given. A two-dimensional decomposition is regarded as a better solution in general for massively parallel computation. This is because a two-dimensionally decomposed domain has fewer interface grids that should make communications with adjacent MPI regions. Since efficient vector operation requires sufficient vector length, inner-loop direction has not been decomposed and kept long enough. Efficiencies are compared between computations with a one-dimensional and two-dimensional decomposition, and the former has turned out to be higher [22]. This is possibly because imbalance of the number of marine/land grids for a two-dimensional decomposition is relatively large in the polygonal domain where the inner-loop direction of a block is designed to extend orthogonally to the coast. Another possible reason is that a two-dimensional decomposition actually increases communication pairs of processes due to the nesting scheme between regions with

Original Code

```
IF(MM(I,J,1)>0.0)THEN
  IF(I>1)THEN
    IF(DM(I-1,J,1)>=GX)THEN
      XDM = MM(I-1,J,1)*MM(I-1,J,1)/DM(I-1,J,1)  #F1
      IF(DZ(I-1,J)<GX)  XDM = 0.0
      IF(DZ(I  ,J)<GX)  XDM = 0.0
    ELSE
      XDM = 0.0
    END IF
    XM = XM - RX*(MM(I,J,1)*MM(I,J,1)/DM(I,J,1)-XDM)
  END IF                                        #F2
ELSE
  IF(DM(I+1,J,1)>=GX)THEN
    XDM = MM(I+1,J,1)*MM(I+1,J,1)/DM(I+1,J,1)  #F1
    IF(DZ(I+2,J)<GX)  XDM = 0.0
    IF(DZ(I+1,J)<GX)  XDM = 0.0
  ELSE
    XDM = 0.0
  END IF
  XM = XM - RX*(XDM-MM(I,J,1)*MM(I,J,1)/DM(I,J,1))
END IF                                          #F2
```

Optimized Code

```
IF (MM(I,J,1)>0.0)THEN
  IIDX = 1
  WDM01 = DM(I-1,J,1)
  WDZ01 = DZ(I-1,J)
  WDZ02 = DZ(I  ,J)
  WM01  = MM(I-1,J,1)
ELSE
  IIDX = -1
  WDM01 = DM(I+1,J,1)
  WDZ01 = DZ(I+2,J)
  WDZ02 = DZ(I+1,J)
  WM01  = MM(I+1,J,1)
END IF

XDM = 0.0
IF(WDM01>=GX.AND.WDZ01>=GX.AND.WDZ02>=GX)THEN
  XDM = WM01 * WM01 / WDM01  #F1
END IF
XM = XM –
     RX*((MM(I,J,1)*MM(I,J,1)/DM(I,J,1))*IIDX-XDM*IIDX)
                                              #F2
```

Fig. 8. Example of vector optimization. The upwind scheme refers to different grid points for each direction of flow but the structure of functions is same. Although the original code is divided into two parts according to the direction of flow and functions F1 and F2 designated with blue color are repeated, it is able to integrate them by preparing for work variables like in the optimized code. Green letters are conditions where the resultant flux ends in zero, which are also organized so that the number of layers is unit.

different resolutions, which is peculiar to tsunami modeling. Further discussions and schematics regarding the dimension of parallelization can be found in the previous work of the authors [22].

Considering the corner of a block where nesting in multiple directions is required, possibly with the same MPI process, the model adopts a device to package all relevant data and send/receive them at one time. In addition, exchange of water levels and fluxes are omitted for a grid whose elevation is above the datum of topography data by shrinking the communication table as one of preprocesses prior to the time integration. In order to facilitate this saving in communication, we have imparted modifications to algorithms regarding exchange of water levels and fluxes, and average of bathymetry/topography data at boundary regions.

2.6. Improvement of Parallelization Efficiency at a Small Number Cores

The number of necessary CPU cores is dependent on the degree of difficulty in a given numerical calculation. For example, a small number of cores are used when the total number of grids is small, sea-bottom slop is gentle and the CFL condition is mild, or a time limit is loose, i.e., not as strict as 10 minutes. The authors constructed polygonally nested grid systems of the highest resolution of 30 meters for 21 regions along Nankai Trough, and clarified that computational efficiency deteriorates when a domain has a complex configuration and consequently lots of blocks, even when but the calculation itself is not difficult [22]. This situation is shown in **Figs. 9(a)–(c)**. In the case of Kochi Prefecture, the CFL condition is milder and the simulation requires a shorter time if many cores are deployed. With a small number of cores, however, the Kochi case takes a long time (32 cores) or even the simulation cannot be conducted (16 cores). This is because each block must accept at least one core. If the total number of cores deployed slightly exceeds the number of blocks, some blocks would have large areas and load distribution does not function well.

In order to overcome this problem, we have improved the new model so that an MPI process is able to deal with a range covering multiple polygonal blocks (**Fig. 10**). The result of computational efficiency is shown in **Fig. 9(d)**. The efficiency at a smaller number of CPU cores has been remarkably ameliorated, and the model has become applicable not only to massively-parallel computation but also to simpler problems, which could be encountered more frequently in the practical situation. Enhancement of grid resolution and speed are not the sole factors that determine the overall accuracy of tsunami inundation forecasting.

In the next section verification and validation of the newly-developed model are discussed, followed by the evaluation of computational efficiency in Section 4.

3. Verification and Validation through Benchmark Problems

3.1. NTHMP Benchmark Problems

Triggered by the catastrophic 2004 Indian Earthquake and Tsunami, the National Tsunami Hazard Mitigation

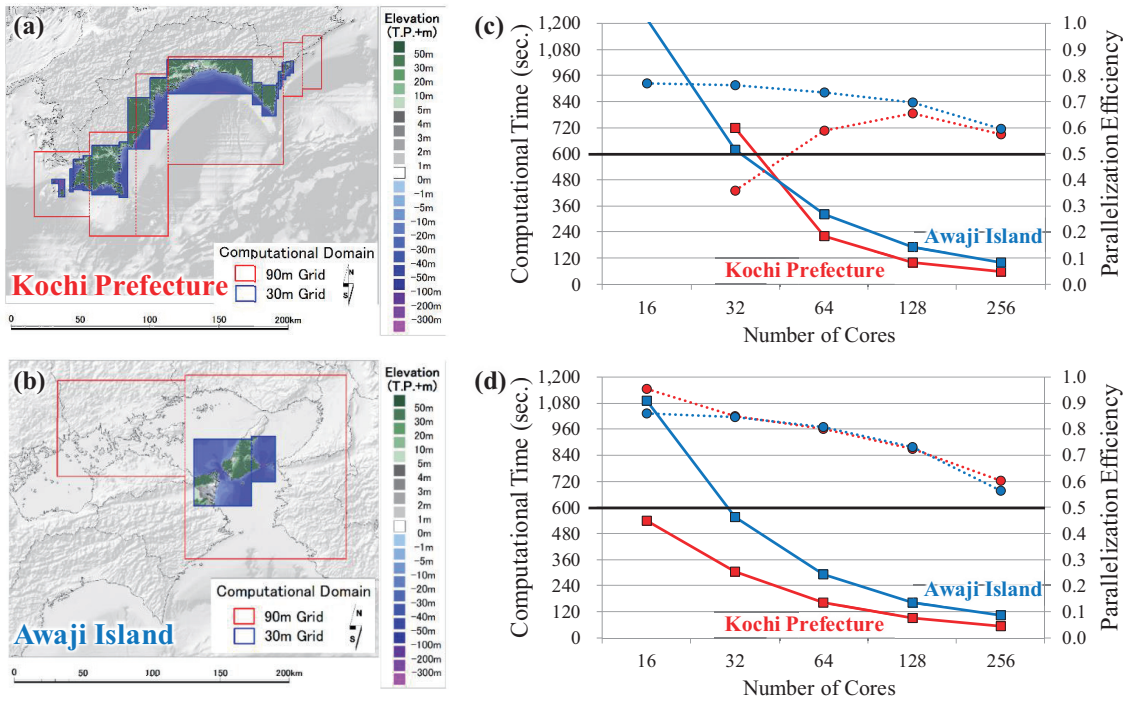

Fig. 9. Configuration of domains for Kochi Prefecture (a) and southern Awaji Island (b), and computational efficiency for the two regions, respectively (c, d). Both domains have almost same number of grids (10 million). The domain (a) consists of 28 blocks including regions with 270- and 810-meter resolutions and its time step is 0.5 second. On the contrary, (b) is formed by 6 blocks and has the time step of 0.25 second. Square symbols in graphs denote computational time, and disks are parallelization efficiency, which is the rate of speed up compared to a single-core calculation normalized by the number of deployed cores. Compared to the graph before the modification (c), the graph (d) after the modification shows clear improvement of efficiency for Kochi Prefecture (red). The computational domain for Kochi Prefecture is defined in the Rectangular Plane IV coordinates, Japanese Geodetic Datum 2000, and that for Awaji Island is in the Rectangular Plane V coordinates, respectively. The datum "T.P." is the mean sea-level of the Tokyo Bay.

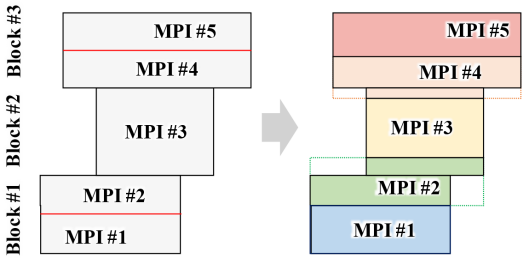

Fig. 10. Schematics of MPI decomposition where a process is allowed to cross borders of blocks. The left image is before modification, and the right image is after the modification, where we see improved load balance. After the modification, memories are also allocated for non-calculated areas designated by dashed lines.

Program (NTHMP), organized by federal agencies and states in the U.S., requires that all operational models for tsunami inundation mapping should be properly validated [21]. In order to ensure a basic level of consistency between efforts to map tsunami inundation, Synolakis et al. [18] proposed a set of benchmark problems (BPs) in 2007. The 2011 NTHMP Model Benchmarking Workshop was held in Galveston, Texas, based on the BPs for cross-comparing different numerical models [19].

The NTHMP BPs contain mainly three categories of problems: analytical, laboratory, and field benchmarking. Some problems deal with a simple condition like a single wave running up on a simple beach, and others deal with a much more complex condition such as tsunami generated by a three-dimensional landslide. What is of critical importance is that each problem is provided with a threshold value of acceptable errors between calculation and either analytical solutions, laboratory measurements, or field observations. For more information on the complete set of BPs, refer to Synolakis et al. [18]. Data for validation can be downloaded from the website of NOAA Center for Tsunami Research [34], or GitHub [35], which includes a short description for each problem.

During the workshop it transpired that some BPs are not applicable to geophysical tsunamis in realistic conditions as a benchmark for a broad spectrum of models: some analytical problems oversimplify the governing equations, and the tsunami generated by a three-dimensional landslide cannot be solved stably by a model with the commonly-used nonlinear shallow water equations (NSWEs) [19]. Therefore, NTHMP discusses that BP #1, BP #4, BP #6, and BP #9, which are shown in

Table 1. List of priority benchmark problems. The threshold values of error are based on NTHMP [19].

Name	Category	Error Threshold	Description
BP #1	Analytical Solution	5%	Single Wave on a Simple Beach
BP #4	Laboratory Experiment	10%	Solitary Wave on a Simple Beach
BP #6	Laboratory Experiment	10%	Solitary Wave on a Conical Island
BP #9	Field Measurement	20%	Okushiri Island Tsunami

Table 1, are priority problems. These problems were actually used for model-comparison in the workshop [19]. We have benchmarked the newly-developed model with these four problems, and the model was successfully validated with errors sufficiently below the thresholds shown in **Table 1**. In this paper, an overview of BP #6 and BP #9 is given for brevity.

3.2. BP #6

This problem is about a three-dimensional laboratory experiment that simulates tsunami behaviors around Babi Island in the 1992 Flores Earthquake and Tsunami. The details of the hydraulic experiment are described in Briggs et al. [36]. The tsunami arrived from the north of the conical island, but the southern side of the island experienced high inundation [37]. In this benchmarking, therefore, modelers are supposed to reproduce this phenomenon where wavefronts split in front of the island and then collide behind it, resulting in high inundation. In addition to this distinctive phenomenon, the time series of the water level and run-up distribution around the island should be compared with the laboratory measurements.

Figure 11(a) shows the basin geometry. The still water depth, d is set to 0.32 m. The horizontal to vertical ratio of the slope of the island is 4 : 1, and the height is 0.625 m. There are three cases according to the initial wave heights H that are normalized by the still water depth d. In case A, H is 0.045; in case B, H is 0.096; in case C, H is 0.181.

The whole extent of the basin shown in **Fig. 11(a)** and is represented by a rectangular domain with a spatial resolution of 0.01 m. A polygonal inner domain with a spatial resolution of $0.01/3$ m is adopted for cases B and C as shown in **Fig. 11(b)**. This is because initial waves in cases B and C have shorter wave periods. Regarding the grid resolution Δx necessary for the proper representation of tsunami run-up, Goto and Shuto [25] propose a condition as follows:

$$\Delta x \alpha g T^2 \leq 4.0 \times 10^{-4}, \quad \ldots\ldots\ldots\ldots \quad (5)$$

where α is the slope of the sea floor, and T is wave period. The incident waveforms are provided at the gauges 1 to 4. For case B, it is inferred from the incident waves that wave period is around 3 seconds, leading to the necessary resolution slightly less than 0.01 m. Although Eq. (5) is applicable to a frictionless case, it is more stringent than a case with bottom friction, and thus the resolution of 0.01 m was regarded as a basis. A time step Δt for each case was chosen so as to suffice the CFL condition, but simulation sometimes became unstable, possibly because the tsunami amplitude is not negligible to the still water depth. Therefore, Δt was lowered until the simulation becomes stable: Δt consequently is 2.0×10^{-3} second for case A, and $1/3 \times 10^{-3}$ second for cases B and C, respectively. In the numerical calculation, the water levels given at the gauges 1 to 4 were interpolated both in time and space, and utilized as incident plane waves, instead of modeling the movement of the wavemaker itself. Manning's roughness coefficient was uniformly set to 0.01 $\mathrm{m}^{-1/3}$s for all grids and cases.

Figure 11(b) shows the distribution of maximum water level for case C. This verifies that the polygonally nested

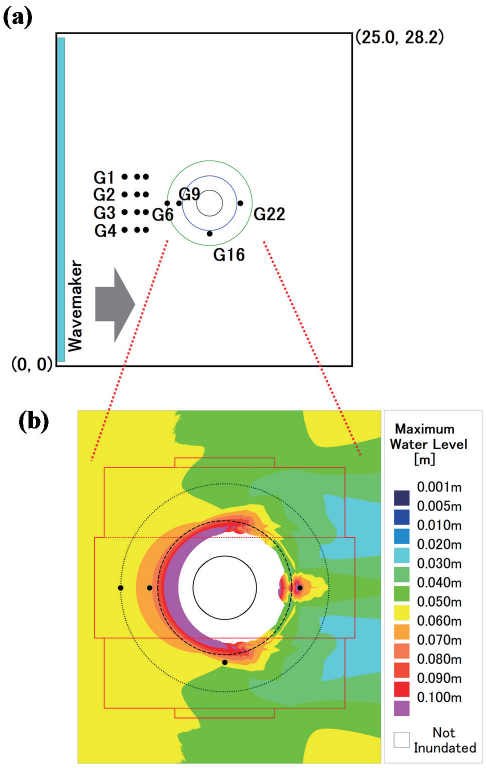

Fig. 11. Schematics of the basin geometry (a) and the polygonal grid system (b) for the BP #6. In the panel (a), the thick black rectangle corresponds to the basin. Circles in black, blue and green denote the crest of the cone, the initial shoreline, and the toe of the cone, respectively. Black disks are gauges for measuring water level, where "G" in the figure means "Gauge." The gauges for incident waves, G1 to G4 are positioned differently for each case: from left to right, they are for the case A to C. The enlarged view (b) shows the polygonal blocks and region constructed in the vicinity of the conical island. Maximum water level for the case C is also shown. Here the initial shoreline and the toe of the cone are designated by a dashed circle and a dotted circle, respectively. The total number of grid points in the rectangular domain is about 7 million, and the grid system including the polygonal inner domain has about 14 million grid points.

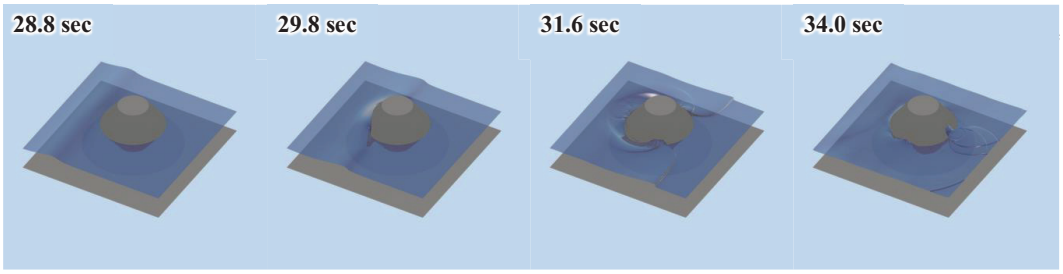

Fig. 12. Snapshots of tsunami propagation and run-up. case C is taken as an example. The figures are vertically magnified by a factor of 5 in comparison with the horizontal plane.

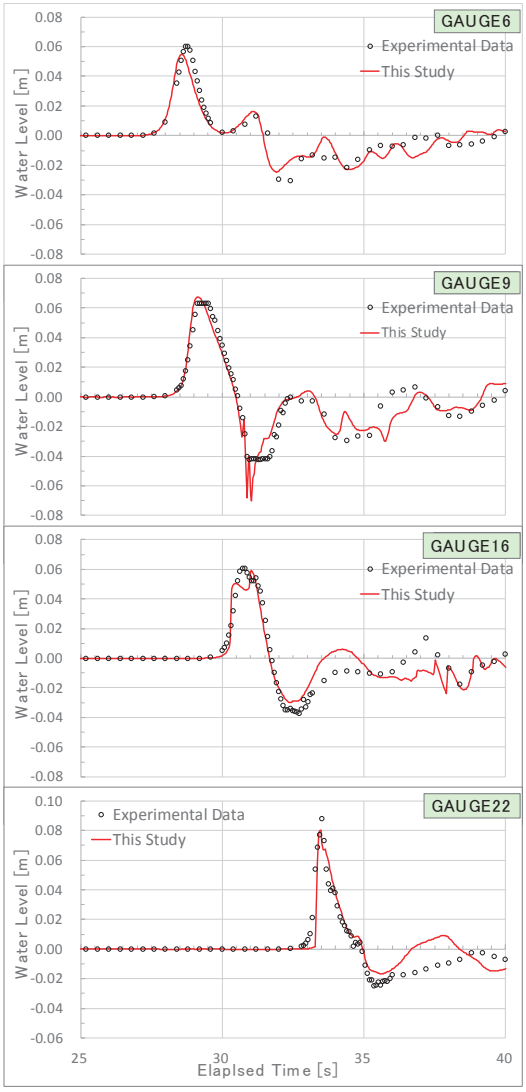

Fig. 13. Time series of water level at four gauges for the case C. For visibility, experimental data are shown either every 10 step (0.4 second) in general, or every 2 step (0.08 second) for rapidly changing parts. The gauge 9 has missing values in the experimental data around the maximum and the minimum.

grid system in BP #6 is able to stably solve NSWEs shown in Eqs. (1) to (3). The snapshots of tsunami propagation and run-up onto the island are shown in **Fig. 12**, also for case C due to limitations of space. This also shows the stability of the simulation in terms of time evolution, as well as the phenomenon of collision of split tsunami waves behind the island.

The comparison of water level dynamics between the simulation and the experiment is given in **Fig. 13**, taking an example of case C. Experimental values are vertically shifted so that the water level is zero at the initial time. The overall appearance resembles between the simulation and the experiment. Since case C deals with a breaking wave, the gauge 9 experiences missing data in the experiment, and temporary instability in the simulation. The phenomenon of so-called "shallow-water steepening" is visible at the gauges 6 and 9, where a modeled wave steepens faster than the physical behavior of tsunami due to lack of dispersive terms. However, this phenomenon is very limited, possibly because in this simulation the grid resolution is made as fine as $0.01/3$ m based on the proposal by Goto and Shuto [25], and the time step is set as large as possible so that the Courant number is kept largest possible. The mean relative error is 7.0% for a maximum, and the mean relative RMS error is 7.6%, both of which are below the allowable threshold of 10% shown in **Table 1**. Here, "relative" means normalization by a maximum in the experiment in the case of an error on maximum wave amplitude or run-up, and by a maximum amplitude (maximum subtracted by minimum) in the case of an RMS error [19].

Regarding maximum run-up, comparison results are shown in **Fig. 14**. The general appearance of run-up distribution is again in good agreement, and an exceptionally high run-up value at the lee side of the island is clearly visible in case B. The relative errors regarding a maximum are 17.5% for case A, 2.6% for the case B, 1.0% for case C, respectively. This results in the mean relative error regarding a maximum of 7.0%, which is below the allowable error of 10%. The mean relative RMS value is 17.7%, but the corresponding RMS values for other eight models in the 2011 workshop are also above the 10% threshold, ranging between 12–22% [19]. This indicates that in benchmarking with this difficult problem, accuracy of the new model is comparative to the accuracy of other operational models, some of which solve higher-order non-hydrostatic equations. Asymmetric dis-

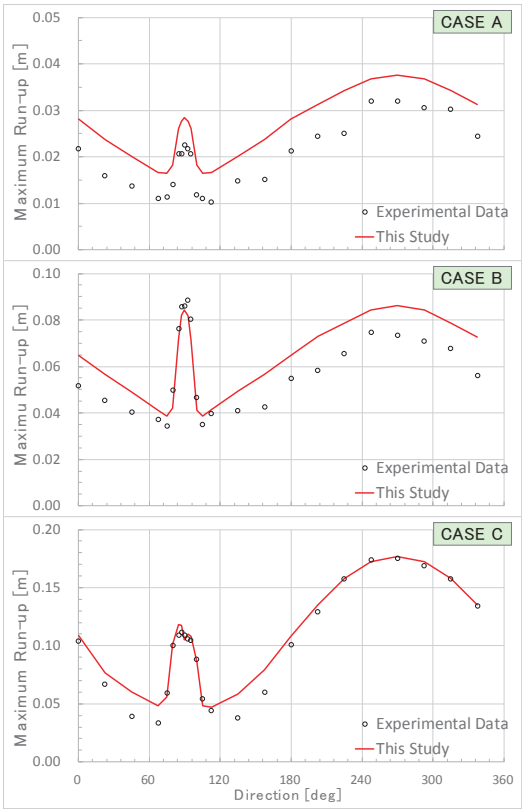

Fig. 14. Maximum run-up distributions for case A (a), case B (b), and case C (c), respectively. The windward side of the island corresponds to the direction of 270°, and the leeward side is 90°.

tributions seen at the opposite side of the island for case C can be attributed to asymmetry in the incident waves, because not only simulation results but also experimental data are distributed in that manner.

3.3. BP #9

The BP #9 provides validation with a geophysical tsunami, namely the 1993 Hokkaido-Nansei-Oki Earthquake and Tsunami (Okushiri tsunami). Although many objectives in this BP exist [35], water level dynamics at two tide stations and maximum run-up values obtained by field measurements are discussed in this paper.

First, it was necessary to deal with a "flaw" [35] in bathymetry/topography data for this problem. It is said that original DEM data provided by Takahashi et al. [38] have significant horizontal and vertical misalignment of grids, and that modified grids have been organized in the latitude-longitude coordinate system by adding and subtracting certain rows and columns at domain boundaries [35]. Since file names of the original DEM grids include the spatial resolution in the unit meter like "D379-687-450m.txt" [34], it can be inferred that the grids are aligned not in the latitude-longitude coordinate system but in some kind of Cartesian coordinate system. By considering the spatial extent and the date of construction of the DEM data, the authors adopted the Rectangular Plane

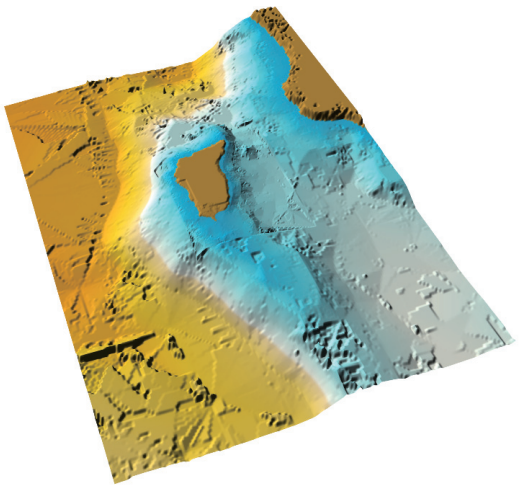

Fig. 15. Configuration of local bathymetry/topography in the vicinity of Okushiri Island compiled from the original DEM data [34]. There is a small difference in elevation, but no misalignment error shown in [35] are visible.

XI coordinate system and Tokyo Datum. It was also assumed that there are lines of extra cells in the original data, as shown in **Fig. 1(b)**. The DEM data as rectangular grids were then successfully overlaid on a GIS without misalignment errors, as shown in **Fig. 15**. The spatial extent of each domain provided in the original data set [34] is specified basically by the unit of arc minute, and there is still a lack of positional accuracy in determination of the exact extent of a grid system. Therefore, a position of each DEM is adjusted on a GIS so that bathymetry/topography data can fit the shoreline public data of the Ministry of Land, Infrastructure, Transport and Tourism [39].

As a tsunami source model, the fault model DCRC-17a consisting of three sub-faults proposed by Takahashi et al. [40] was used, instead of reading the initial sea surface data provided in the data set for benchmarking [35]. A one-stop tsunami simulation from a fault model is facilitated by the enhanced functionality of the new model as described in Section 2.

A polygonally nested grid system is also adopted for this problem as shown in **Fig. 16**. Since a polygonal domain is able to efficiently cover a wider area, the domain with the spatial resolution of 50 meters are extended so that entire Okushiri Island can be contained, as shown in **Fig. 16(b)**. Moreover, domains with other resolutions are also extended in order to use finer grids and to avoid setting domain boundaries at coastal lowlands. Although the island is covered by three grids of 150-meter resolution in the original grid system, and consequently simulation must be repeated three times, evaluation of tsunami inundation of Okushiri tsunami has become much more efficient using the new model. Manning's roughness coefficient was uniformly set to 0.025 $m^{-1/3}s$ for all grids.

In **Fig. 16(a)**, the positions of the Iwanai tide gauge and the Esashi tide gauge are also shown. Among the survey

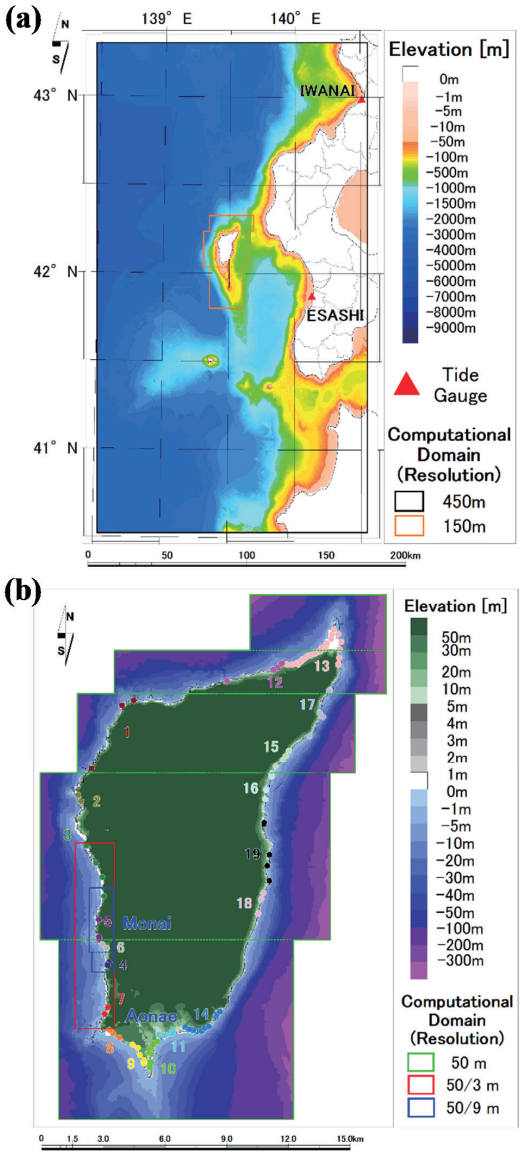

Fig. 16. Schematics of the polygonally nested grid system and the problem establishment for offshore areas (a), and coastal areas (b). Tsunami survey data are shown as disks in the panel (b), whose colors correspond to the designated region numbers that are defined in NTHMP [19]. The classification of survey data into the 19 regions was conducted based on proximity. The time step is set to 0.2 second according to the CFL condition. The number of grid points amounts to less than one million.

data of tsunami inundation, which are provided in the data set for benchmarking [35], only the data collected by a survey team of Tohoku University are used for the sake of the integrity of the data. Neglecting one entry with missing inundation depth, the total number of observations is 124. They are shown in **Fig. 16(b)** with the region numbers defined in the NTHMP [19]. Since the DEM data are horizontally shifted on the basis of the shoreline data, field observation data are also moved by a couple of hundred meters at maximum according to the local topography.

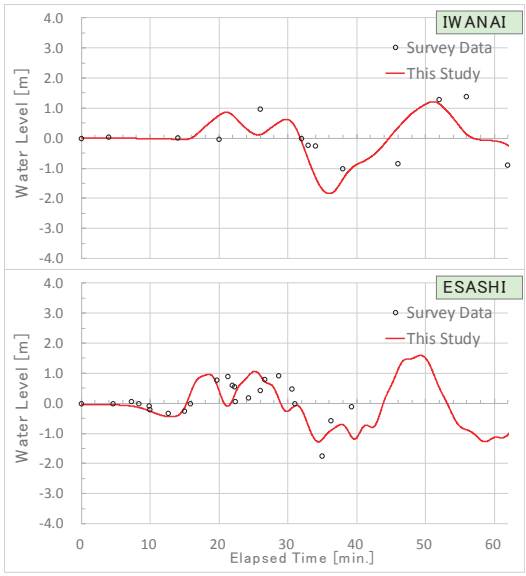

Fig. 17. Time series of water level at the two tide gauges. A moving average filter of 5 minutes is imposed on simulation results for Iwanai, considering the frequency of the observation. For Esashi a corresponding time window of a filter is 2 minutes.

Figure 17 shows the comparison of simulation and field measurements in terms of water surface dynamics. A general time series is in good agreement. The mean relative error on a maximum is 14.1%, which is below the threshold value of 20% in **Table 1**. The mean relative RMS error is 23.1%, which exceeds the threshold value. In the NTHMP [19], however, no quantitative evaluation is conducted in terms of RMS errors. NTHMP argues that the complex port layout around the Iwanai station is not well resolved in the bathymetry/topography data and that there would be inaccuracy in the initial condition [19]. Paying attention only to the Esashi data in this study yields a relative error on a maximum of 15.0%, and a relative RMS error of 17.2%, both of which are below the threshold. A cross-comparison of numerical models seems difficult for this BP #9 because it is said that several models suffered from the above-mentioned challenge regarding the original DEM data and results shown in the proceeding of the workshop considerably vary from one model to another [19].

The comparison of maximum run-up is shown in **Fig. 18** and **Table 2**. The figure indicates that the overall distribution of maximum run-up averaged within each region is reproduced well in simulation, but maximum tsunami height is underestimated in several regions. The most outstanding example is region 5, which corresponds to the Monai area shown in **Fig. 16(b)**. As shown in **Table 2**, the maximum run-up height is 31.70 m in the field measurement. On the contrary, it is 17.98 m in the simulation. From the viewpoint of cross-comparison of numerical models, many models tested in the 2011 workshop also fail to reproduce the local maximum run-up as high as 31.7 m in the Monai area [19]. They argue that this un-

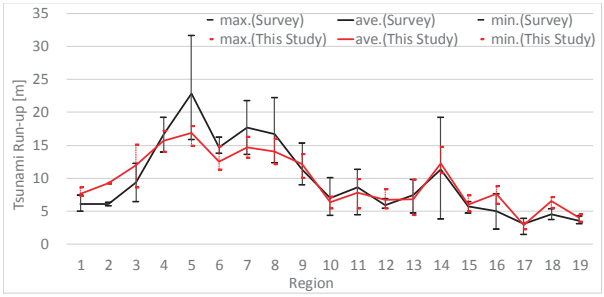

Fig. 18. Maximum run-up distributions organized in the 19 regions. The locations and division of regions are shown in **Fig. 16(b)**.

Table 2. List of run-up errors around Okushiri Island organized in 19 regions. "ERR" is relative error on run-up defined in NTHMP [19].

region	ERR	sample	Survey Data [m]			This Study [m]		
#	[%]	#	min.	max.	ave.	min.	max.	ave.
1	15.8	6	4.94	7.40	6.09	7.31	8.57	7.63
2	47.0	2	5.78	6.32	6.05	9.13	9.29	9.21
3	0.0	4	6.41	12.22	9.31	8.58	15.16	11.97
4	0.0	2	13.95	19.25	16.60	14.05	17 26	15.66
5	0.0	6	15.88	31.70	22.84	14.99	17.98	16.89
6	8 2	3	13.74	16.19	14.65	11.3	14.87	12.49
7	0.0	2	13.62	21.80	17.71	13.1	16.30	14.70
8	0.0	3	12.35	22.21	16.68	12.12	16.08	14.01
9	0.0	6	8.95	15.36	11.34	10.05	13.68	12.15
10	0.0	15	4.30	10.06	6.95	5.4	7.24	6.29
11	0.0	5	4.45	11.30	8.57	5.41	9.88	7.79
12	0.0	4	5.41	6.83	5.90	5.44	8.36	6.68
13	0.0	29	4.67	9.79	7.43	4.46	9.82	6.80
14	0.0	15	3.81	19.21	11.30	10.75	14.75	12.24
15	0.0	4	4.68	6.45	5.71	4.99	7.42	5.97
16	0.0	4	2.25	7.58	4.94	6.17	8.74	7.56
17	0.0	5	1.40	3.85	3.07	2.21	3.26	2.87
18	32.8	4	3.73	5.36	4.55	5.55	7.12	6.50
19	0.0	5	3.06	4.25	3.55	3.38	4.54	3.95
Mean:	5.5							

derestimation could be explained either by lack of accuracy in the topography data, or by uncertainties in the initial water fluctuation, or by possible vertical movement of the tsunami that current models cannot reproduce [19]. In terms of a quantitative evaluation of run-up, NTHMP [19] adopts an error formula for multiple field measurements in a specific region. Since the formula is not very common, it is explained as follows. Let us denote a minimum run-up value in multiple field observations as

$$\zeta^{\mathrm{o}}_{\mathrm{min}} = \min_i \zeta^{\mathrm{o}}_i, \quad \ldots\ldots\ldots\ldots\ldots\ldots \quad (6)$$

where i indicates each observation value and "o" means observation. A maximum run-up value is then written as $\zeta^{\mathrm{o}}_{\mathrm{max}}$, and an average is written as $\zeta^{\mathrm{o}}_{\mathrm{ave}}$, respectively. Here, a run-up value obtained by a numerical model is specified by the letter "m" instead of the letter "o," e.g., $\zeta^{\mathrm{m}}_{\mathrm{ave}}$, for an average in the region. The formula for a relative error in a specific region, *ERR*, is defined as zero if $\zeta^{\mathrm{o}}_{\mathrm{min}} \leq \zeta^{\mathrm{m}}_{\mathrm{ave}} \leq \zeta^{\mathrm{o}}_{\mathrm{max}}$. Otherwise,

$$ERR = \frac{\min \begin{bmatrix} \mathrm{abs}\left(\zeta^{\mathrm{o}}_{\mathrm{min}} - \zeta^{\mathrm{m}}_{\mathrm{min}}\right), \\ \mathrm{abs}\left(\zeta^{\mathrm{o}}_{\mathrm{ave}} - \zeta^{\mathrm{m}}_{\mathrm{ave}}\right), \\ \mathrm{abs}\left(\zeta^{\mathrm{o}}_{\mathrm{max}} - \zeta^{\mathrm{m}}_{\mathrm{max}}\right) \end{bmatrix}}{D}, \quad \ldots\ldots \quad (7)$$

where the denominator D is selected from the following observational values $\left[\zeta^{\mathrm{o}}_{\mathrm{min}}, \zeta^{\mathrm{o}}_{\mathrm{ave}}, \zeta^{\mathrm{o}}_{\mathrm{max}}\right]$, according to the value selected as the minimum in the numerator. The results regarding this relative error, *ERR*, are given in **Table 2** for the same 19 regions. The average error is 5.5%, which is sufficiently lower than the acceptable threshold of 20%.

As mentioned above, the new model has also been validated using a case of a geophysical tsunami with sufficient accuracy.

4. Case Studies of Real-time Tsunami Inundation Simulation for the Entire Nankai Trough Region

4.1. Feasibility of 10-10-10 Challenge

In this subsection, we discuss the feasibility of real-time tsunami simulation with 10-meter grid resolution within 10 minutes on a regional scale. The newly-developed tsunami inundation model is computationally efficient due to a polygonally nested grid system and has been validated through the NTHMP BPs. The model is named the "Real-time Tsunami inundation (RTi) model."

A vector supercomputer installed at Tohoku University is utilized as an HPC resource for performance evaluation of the SX-ACE. This is not only because the SX-ACE has proven to perform well in memory-intensive tsunami inundation simulations, but also because the SX-ACE system is equipped with an emergency job, which suspends already-running jobs in order to execute a pressing and important job like tsunami simulation immediately after earthquake occurrence on a priority basis [13]. Osaka University, located about 600 km away from Tohoku University, operates a supercomputer system based on the same SX-ACE, and it is also possible to construct a regionally multiplexing disaster system [23]. Moreover, the authors, in collaboration with other researchers and private enterprises, organize the Association for Real-time Tsunami Science (ARTS), which has, since 2014, promoted research and social implementation of real-time tsunami forecasting based on industry-academia collaboration, using the SX-ACE systems.

The computational performance is evaluated, taking an example of the case of Kochi Prefecture, whose domain is shown in **Fig. 5(b)**. The length of the coastline in Kochi Prefecture is about 700 km. The time required for a 6-hour tsunami inundation simulation is shown in **Fig. 19**, for each number of CPU cores used in the computation. The simulation using 128 cores requires 599 seconds. In the previous study [15], it is elucidated that 1,536 cores

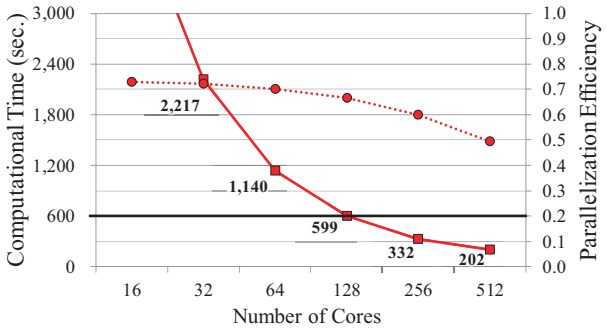

Fig. 19. Computational performance of the RTi model for the 10-meter resolution case of Kochi Prefecture. Square symbols denote computational time, and disks are parallelization efficiency, which is the rate of speed up compared to a single-core calculation normalized by the number of deployed cores.

of the SX-ACE were required for the same spatial extent by a set of rectangular systems as shown in **Fig. 5(a)**. The RTi model is over 10 times as more efficient than the conventional tsunami model. It can also be inferred from the ratio of improvement in efficiency that 2,451 cores of the SX-ACE are the overall computational resources needed for real-time tsunami inundation forecast on the whole coastal region along the Nankai Trough subduction zone if the RTi model is used. The extensive coastal region is designated as areas enclosed by 90-meter domains (red polygons) in **Fig. 6**. As each node of the SX-ACE has four cores and a computational performance of 276 Gflop/s, the required resources correspond to a computational performance of about 170 Tflop/s. Since Tohoku University operates 2,560 nodes (10,240 cores) of the SX-ACE, the required resources for the entire Nankai Trough region are equivalent to no more than 24% of all the SX-ACE. This indicates that real-time tsunami inundation forecast on a regional scale is indeed feasible. In other words, the 10-10-10 challenge in real-time tsunami inundation forecasting can be achieved by using the RTi model with the existing HPCI.

4.2. Disaster Information System of Japan's Cabinet Office

The Disaster Information System (DIS) operated by the Cabinet Office of the Japanese Government estimates earthquake-induced damage immediately after a natural disaster for efficient disaster response. The system was introduced to the Government following the 1995 Great Hanshin-Awaji Earthquake, and actually succeeded in the rapid estimation of immense damage in the case of the 2011 Great East Japan Earthquake. However, estimated damage concentrated more on inland areas than in the coastal areas that were primarily devastated by tsunamis. This is because at that time the DIS did not have a function for estimating tsunami-induced damage. Learning from the experience in the 2011 event, and considering the imminent risk of a huge earthquake in the Nankai Trough subduction zone, the Government has included a function of tsunami damage estimation as a subsystem of DIS since 2017. Previously, there existed no comparable system because damage estimation of tsunami for broad areas like the entire Nankai Trough region used to be infeasible due to the computational costs of two-dimensional simulations of tsunami inundation. Accordingly, the RTi model was incorporated into the tsunami subsystem for the sake of efficient estimation of tsunami inundation and damage on a regional scale.

The coverage of estimation is from Kagoshima Prefecture to Shizuoka Prefecture, which has coastlines of about 6,000 km. Since the objective is to grasp a whole picture of tsunami damage within 30 minutes after earthquake occurrence, and to utilize the information for disaster response of the Japanese Government, the spatial resolution is set to 30 meters. However, the time allotted to a single execution of tsunami inundation simulation and damage estimation from a fault model is merely 4.5 minutes (270 seconds), and thus this use-case is also computationally demanding. The reasons for the considerably tight time limit are as follows. Firstly, the tsunami system must conduct multiple simulations for an earthquake event based on multiple fault models that will include reliable GNSS-based models, considering uncertainties in the estimation of fault models. For further information on the GNSS-based model in tsunami forecasting, refer to Ohta et al. [41]. Secondly, it also takes time for reliable fault estimation, especially in the event of a huge tsunamigenic earthquake whose fault rupture would possibly continue for a while. Finally, it is time-consuming to visualize simulation results on a GIS, to compile estimated tsunami damage in a report, and to disseminate the information to disaster responders via a network.

For this system, which is actually in operation in a redundant manner by using the supercomputer systems at Tohoku University and at Osaka University, 239 nodes (956 cores) of the SX-ACE are deployed and damage estimation of tsunami is conducted when a tsunamigenic earthquake occurs near Nanaki Trough.

5. Conclusions

This paper describes the development of a new tsunami inundation model, namely the RTi model, in terms of both enhanced functions for estimating inundation and damage, and of improved efficiency in computation. The model has been benchmarked through the NTHMP problems widely used in the U.S. and successfully validated. As mentioned in the case studies, the RTi model has realized real-time tsunami inundation forecasting on a regional scale.

Although discussion here is focused on real-time tsunami simulation on a supercomputer system, the RTi model is able to complete "faster than real-time" tsunami inundation simulation on an ordinary workstation due to its high efficiency. For example, Musa et al. [40] examine performance of the model by using a workstation with the

many-core architecture, Intel Xeon Phi, and shows that it takes only 2.7 hours for a single node of Xeon Phi machine to conduct 6-hour time integration in the case of Kochi Prefecture discussed in Section 4.1. A real-time forward simulation without HPCI will facilitate implementation in cases in which a forecasting system based on HPCI is limited in terms of cost, networking, or security.

Due to the high computational efficiency on a wider scale, moreover, the RTi model is versatile in that it is useful also for creating a database of tsunami inundation. An inundation database can be then applied to probabilistic tsunami hazard assessment on land for instance. Another advantage of the model is that it is a model for forward simulation. It can become higher-functioning, higher-precision, and of course faster by incorporating the latest knowledge from research communities of tsunami engineering, geophysics, and computational science. It is also possible for a forward numerical model to promptly handle the latest BPs for the sake of improving accuracy and obtaining further social confidence. In fact, model benchmarking is to be a continuous process, as Horrillo et al. argue [21].

In terms of future prospects, we intend to extend the technology of real-time tsunami inundation forecasting to cover far-field tsunamis in addition to the near-field tsunami discussed in this paper, and/or other natural hazards such as storm surges and flooding, contributing further to society in terms of disaster mitigation. We expect that disaster response activities will be better managed based on rich and unprecedented disaster information, such as forecasted distributions of inundation depth and predicted damage to persons and properties.

Acknowledgements

The authors thank Mr. Takayuki Suzuki, Mr. Yasuhiro Murata, and Mr. Atsushi Tanobe at Kokusai Kogyo Co., Ltd. for their assistance and useful comments in the model development. We also show our appreciation to Mr. Kenji Oizumi at the Cyberscience Center at Tohoku University and Mr. Yoshihiko Sato at NEC Solution Innovators, Ltd. for their support in the allocation of computational resources. We greatly appreciate the extensive discussion on tsunami source models with Prof. Hino and Assoc. Prof. Ohta at Graduate School of Science, Tohoku University. This study is partially supported by the JST CREST Grant Number JPMJCR1411, Japan. This research is also partially supported by Grants-in-Aid for Scientific Research(C) #18K11322, by the Joint Usage/Research Center for Interdisciplinary Largescale Information Infrastructures in Japan (Project ID: jh180040-NAH), and by the Ministry of Education, Culture, Sports, Science and Technology of Japan (Next Generation High-Performance Computing Infrastructures and Applications R&D Program). In this study, the SX-ACE systems of the Cyberscience Center at Tohoku University and the Cybermedia Center at Osaka University were utilized. We express our sincere gratitude to two anonymous reviewers for their helpful comments, and to the editors for their assistance in publication.

References:

[1] M. Numada, M. Inoue, and K. Meguro, "Framework of disaster responses based on the analysis of the 2011 Great East Japan Earthquake disaster, the 2015 Kanto-Tohoku heavy rain disaster and the 2016 Kumamoto earthquake disaster," J. of Japan Society of Civil Engineers, Series A1 (Structural Engineering & Earthquake Engineering), Vol.73, No.4, pp. 258-269, 2017 (in Japanese with English title and abstract).

[2] Y. Murashima, F. Imamura, H. Takeuchi, T. Suzuki, K. Yoshida, M. Yamazaki, and K. Matsuda, "Adaptability of the aircraft-mounted laser data in tsunami inundation forecast," Proc. of Coastal Engineering, Japan Society of Civil Engineers, Vol.53, pp. 1336-1340, 2006 (in Japanese).

[3] Water and Disaster Management Bureau, and National Institute for Land and Infrastructure Management, Ministry of Land, Infrastructure, Transport and Tourism, "A guide for assesement of tsunami inundation ver. 2.00," 2012, www.mlit.go.jp/river/shishin_guideline/bousai/saigai/tsunami/shinsui_settei.pdf [accessed October 11, 2018] (in Japanese)

[4] N. Takahashi, K. Imai, M. Ishibashi, K. Sueki, R. Obayashi, T. Tanabe, F. Tamazawa, T. Baba, and Y. Kaneda, "Real-time tsunami prediction system using DONET," J. Disaster Res., Vol.12, No.4, pp. 766-774, 2017.

[5] N. Yamamoto, S. Aoi, K. Hirata, W. Suzuki, T. Kunugi, and H. Nakamura, "Multi-index method using offshore ocean-bottom pressure data for real-time tsunami forecast," Earth, Planets and Space, Vol.68, No.128, doi: 10.1186/s40623-016-0500-7, 2016.

[6] A. R. Gusman, Y. Tanioka, B. T. MacInnes, and H. Tsushima, "A methodology for near-field tsunami inundation forecasting: application to the 2011 Tohoku tsunami," J. Geophys. Res. Solid Earth, Vol.119, pp. 8186-8206, doi: 10.1002/2014JB010958, 2014.

[7] T. Baba, N. Takahashi, and Y. Kaneda, "Near-field tsunami amplification factors in the Kii Peninsula, Japan for Dence Ocean Network for Earthquake and Tsunamis (DONET)," Mar. Geophys. Res., Vol.35, pp. 319-325, 2014.

[8] S. Kawamoto, K. Miyagawa, T. Yahagi, M. Todoriki, T. Nishimura, Y. Ohta, R. Hino, and S. Miura, "Development and assessment of real-time fault model estimation routines in the GEONET real-time processing system," M. Hashimoto (Eds.), Int. Symp. on Geodesy for Earthquake and Natural Hazards (GENAH), International Association of Geodesy Symposia, Vol.145, Springer, Cham, doi: 10.1007/1345_2015_49, 2015.

[9] H. Tsushima, R. Hino, H. Fujimoto, Y. Tanioka, and F. Imamura, "Near-field tsunami forecasting from cabled ocean bottom pressure data," J. Geophys. Res., Vol.114, B06309, 2009.

[10] H. Tsushima, R. Hino, Y. Ohta, T. Iinuma, and S. Miura, "tFISH/RAPiD: rapid improvement of near-field tsunami forecasting based on offshore tsunami data by incorporating onshore GNSS data," Geophys. Res. Lett., Vol.41, doi: 10.1002/2014GL059863, 2014.

[11] Y. Oishi, F. Imamura, and D. Sugawara, "Near-field tsunami inundation forecast using the parallel TUNAMI-N2 model: application to the 2011 Tohoku-Oki earthquake combined with source inversions, Geophys. Res. Lett., Vol.42, doi: 10.1002/2014GL062577, 2015.

[12] A. Musa, H. Matsuoka, O. Watanabe, Y. Murashima, S. Koshimura, R. Hino, Y. Ohta, and H. Kobayashi, "A real-time tsunami inundation forecast system for tsunami disaster prevention and mitigation," The Int. Conf. for High Performance Computing, Networking, Storage and Analysis (SC15), Austin, Texas, 2015, sc15.supercomputing.org/sites/all/themes/SC15images/tech_poster/poster_files/post142s2-file3.pdf [accessed October 11, 2018]

[13] A. Musa, O. Watanabe, H. Matsuoka, H. Hokari, T. Inoue, Y. Murashima, Y. Ohta, R. Hino, S. Koshimura, and H. Kobayashi, "Real-time tsunami inundation forecast system for tsunami disaster prevention and mitigation," The J. of Supercomputing, Vol.74, No.7, p. 3093, 2018.

[14] S. Koshimura, "Fusion of real-time disaster simulation and big data assimilation – recent progress," J. Disaster Res., Vol.12, No.2, pp. 226-232, 2017.

[15] T. Inoue, T. Abe, S. Koshimura, A. Musa, Y. Murashima, and H. Kobayashi, "Improvement of efficiency of wide-area tsunami simulation through polygonal regions and MPI-parallelization," J. of Japan Society of Civil Engineers, Series B2 (Coastal Engineering), Vol.72, No.2, pp. 373-378, 2016 (in Japanese with English title and abstract).

[16] The Investigative Commmission on Massive Earthquake Models in Nankai Trough, 2012, www.bousai.go.jp/jishin/nankai/model/data_teikyou.html [accessed October 11, 2018] (in Japanese)

[17] I. Babuska and J. T. Oden, "Verification and validation in computational engineering and science: basic concepts," Computer Methods in Applied Mechanics and Engineering, Vol.193, Issues 36-38, pp. 4057-4066, 2004.

[18] C. E. Synolakis, E. N. Bernard, V. V. Titov, U. Kanoglu, and F. O. Gonzalez, "Standards, criteria, and procedures for NOAA evaluation of tsunami numerical models," NOAA Technical Memorandum OAR PMEL-135, 2007.

[19] National Tsunami Hazard Mitigation Program, "Proceedings and results of the 2011 NTHMP model benchmarking workshop," NOAA Special Report, 2012, nws.weather.gov/nthmp/documents/nthmpWorkshopProcMerged.pdf [accessed October 11, 2018]

[20] P. J. Lynett, K. Gately, D. Nicolsky, and R. Wilson, "Proceedings and results of the National Tsunami Hazard Mitigation Program 2015 tsunami current modeling workshop," 2017, nws.weather.gov/nthmp/documents/NTHMP_Currents_Workshop_Report.pdf [accessed October 11, 2018]

[21] J. Horrillo, S.T. Grilli, D. Nicolsky, V. Roeber, and J. Zhang, "Performance benchmarking tsunami models for NTHMP's inundation mapping activities," Pure Appl. Geophys., doi: 10.1007/s00024-014-0891-y, 2014.

[22] T. Inoue, T. Abe, S. Koshimura, A. Musa, Y. Murashima, and H. Kobayashi, "A study on applicability of a tsunami inundation model with the polygonally nested grid system and its MPI-parallelization to nation-wide tsunami forecast at multiple grid resolutions," J. of Japan Society of Civil Engineers, Series B2 (Coastal Engineering), Vol.73, No.2, pp. 319-324, 2017 (in Japanese with English title and abstract).

[23] A. Musa, T. Abe, T. Inoue, H. Hokari, Y. Murashima, Y. Kido, S. Date, S. Shimojo, S. Koshimura, and H. Kobayashi, "A real-time tsunami inundation forecast system using vector supercomputer SX-ACE," J. Disaster Res., Vol.13, No.2, pp. 234-244, 2018.

[24] J. J. Dronkers, "Tidal computations: in rivers and coastal waters," Elsevier Science Publishing, USA, 1964.

[25] C. Goto and N. Shuto, "Numerical simulation of tsunami propagations," K. Iida and T. Iwasaki (eds.), Tsunamis – Their science and engineering, Terra Scientific Publishing Company, Tokyo, pp. 439-451, 1983.

[26] C. Goto, Y. Ogawa, N. Shuto, and F. Imamura, "IUGG/IOC Time project: numerical method of tsunami simulation with the leap-frog scheme," IOC Manuals and Guides, No.35, UNESCO, 1997.

[27] F. Imamura and C. Goto, "Truncation error in numerical tsunami simulation by the finite difference method," Coastal Engineering in Japan, Vol.31, No.2, pp. 245-263, 1988.

[28] F. Imamura, "Review of tsunami simulation with a finite difference method," H. Yeh, P. Liu, and C. Synolakis (Eds.), Long-Wave Runup Models, pp. 25-42, World Scientific Publishing, 1995.

[29] Y. Okada, "Internal deformation due to shear and tensile faults in a half-space," Bulletin of the Seismological Society of America, Vol.82, No.2, pp. 1018-1040, 1992.

[30] T. Inoue, Y. Ohta, S. Koshimura, R. Hino, S. Kawamoto, Y. Hiyama, and Y. Doke, "A study on methods for applying fault models rapidly estimated using real-time GNSS to tsunami simulation," J. of Japan Society of Civil Engineers, Series B2 (Coastal Engineering), Vol.72, No.2, pp. 355-360, 2016 (in Japanese with English title and abstract).

[31] Y. Tanioka and K. Satake, "Tsunami generation by horizontal displacement of ocean bottom," Geophysical Research Letters, Vol.23, pp. 861-864, 1996.

[32] K. Kajiura, "The leading wave of a tsunami," Bulletin of the Earthquake Research Institute, Vol.41, pp. 535-571, 1963.

[33] S. Koshimura, T. Oie, H. Yanagisawa, and F. Imamura, "Developing fragility functions for tsunami damage estimation using numerical model and post-tsunami data from Banda Aceh, Indonesia," Coastal Engineering J., JSCE, Vol.51, No.3, pp. 243-273, 2009.

[34] nctr.pmel.noaa.gov/benchmark/index.html [accessed October 11, 2018]

[35] github.com/rjleveque/nthmp-benchmark-problems [accessed October 11, 2018]

[36] M. J. Briggs, C. E. Synolakis, G. S. Harkins, and D. Green, "Laboratory experiments of tsunami runup on a circular island," Pure Appl. Geophys., Vol.144, pp. 569-593, 1995.

[37] H. Yeh, P. F. Liu, M. Briggs, and C. E. Synolakis, "Tsunami catastrophe in Babi Island," Nature, Vol.372, pp. 6503-6508, 1994.

[38] T. Takahashi, "Benchmark problem 4. The 1993 Okushiri tsunami – data, conditions, and phenomena," H. Yeh, P. Liu, and C. Synolakis (Eds.), Long-Wave Runup Models, pp. 384-403, World Scientific Publishing, 1995.

[39] http://nlftp.mlit.go.jp/ksj-e/index.html [accessed October 11, 2018]

[40] T. Takahashi, T. Takahashi, N. Shuto, F. Imamura, and M. Oritz, "Source models for the 1993 Hokkaido Nansei-Oki earthquake tsunami," Pure Appl. Geophys., Vol.144, pp. 747-767, 1995.

[41] Y. Ohta, T. Inoue, S. Koshimura, S. Kawamoto, and R. Hino, "Role of real-time GNSS in near-field tsunami forecasting," J. Disaster Res., Vol.13, No.3, pp. 453-459, 2018.

Name:
Takuya Inoue

Affiliation:
International Research Institute of Disaster Science, Tohoku University
Kokusai Kogyo Co., Ltd.

Address:
468-1 Aramaki Aza Aoba, Aoba-ku, Sendai, Miyagi 980-0845, Japan

Brief Career:
2011 Master of Science, University of Cologne
2012- Joined Kokusai Kogyo Co., Ltd.
2015- Doctoral Student, Tohoku University

Selected Publications:
• "A Study on Applicability of a Tsunami Inundation Model with the Polygonally Nested Grid System and its MPI-Parallelization to Nation-wide Tsunami Forecast at Multiple Grid Resolutions," J. of Japan Society of Civil Engineers, Series B, Vol.73, No.2, pp. I_319-I_324, 2017.

Academic Societies & Scientific Organizations:
• Japan Society of Civil Engineers (JSCE)

Name:
Takashi Abe

Affiliation:
International Research Institute of Disaster Science, Tohoku University

Address:
468-1 Aramaki Aza Aoba, Aoba-ku, Sendai, Miyagi 980-0845, Japan

Brief Career:
1990- Joined Tohoku NEC Software, Ltd.
2015- Project Researcher, International Research Institute of Disaster Science, Tohoku University

Selected Publications:
• "A Study on Applicability of a Tsunami Inundation Model with the Polygonally Nested Grid System and its MPI-Parallelization to Nation-wide Tsunami Forecast at Multiple Grid Resolutions," J. of Japan Society of Civil Engineers, Series B, Vol.73, No.2, pp. I_319-I_324, 2017.

Name:
Shunichi Koshimura

Affiliation:
Professor, International Research Institute of Disaster Science, Tohoku University

Address:
468-1 Aramaki Aza Aoba, Aoba-ku, Sendai, Miyagi 980-0845, Japan

Brief Career:
2000-2002 JSPS Research Fellow
2002-2005 Research Scientist, Disaster Reduction and Human Renovation Institute
2005-2012 Associate Professor, Graduate School of Engineering, Tohoku University
2012- Professor, International Research Institute of Disaster Science, Tohoku University

Selected Publications:
• Y. Bai, C. Gao, S. Singh, M. Koch, B. Adriano, E. Mas, and S. Koshimura, "A Framework of Rapid Regional Tsunami Damage Recognition From Post-event TerraSAR-X Imagery Using Deep Neural Networks," IEEE Geoscience and Remote Sensing Letters, Vol.15, No.1, 2018.
• S. Koshimura, "Fusion of real-time disaster simulation and big data assimilation – Recent progress," J. Disaster Res., Vol.12, pp. 226-232, doi: 10.20965/jdr.2017.p0226, 2017.
• Y. Bai, B. Adriano, E. Mas, and S. Koshimura, "Machine Learning Based Building Damage Mapping from the ALOS-2/PALSAR-2 SAR Imagery: Case Study of 2016 Kumamoto Earthquake," J. Disaster Res., Vol.12, No.sp, pp. 646-655, doi: 10.20965/jdr.2017.p0646, 2017.

Academic Societies & Scientific Organizations:
• Japan Society of Civil Engineers (JSCE)
• Institute of Social Safety Science (ISSS)
• Japan Society for Computational Engineering and Science (JSCES)
• Japan Association for Earthquake Engineering (JAEE)
• American Geophysical Union (AGU)

Name:
Akihiro Musa

Affiliation:
Visiting Professor, Cyberscience Center, Tohoku University
Executive Specialist, 1st Government and Public Solutions Division, NEC Corporation

Address:
6-3 Aramaki Aza Aoba, Aoba-ku, Sendai, Miyagi 980-8578, Japan

Brief Career:
1988- NEC Corporation
2014- Visiting Professor, Tohoku University
2018- RTi-cast Inc.

Selected Publications:
• A. Musa, O. Watanabe, H. Matsuoka, H. Hokari, T. Inoue, Y. Murashima, Y. Ohta, R.Hino, S. Koshimura, and H. Kobayashi, "Real-time tsunami inundation forecast system for tsunami disaster prevention and mitigation," J. of Supercomputing, doi: 10.1007/s11227-018-2363-0, 2018.
• R. Egawa, K. Komatsu, S. Momose, Y. Isobe, A. Musa, H. Takizawa, and H. Kobayashi, "Potential of a Modern Vector Supercomputer for Practical Applications – Performance Evaluation of SX-ACE –," The J. of Supercomputing, doi: 10.1007/s11227-017-1993-y, 2017.

Academic Societies & Scientific Organizations:
• Physical Society of Japan (JPS)
• Information Processing Society of Japan (IPSJ)

Name:
Yoichi Murashima

Affiliation:
Project Professor, International Research Institute of Disaster Science, Tohoku University
Chief Executive Officer, RTi-cast Inc.
Kokusai Kogyo Co., Ltd.

Address:
468-1 Aramaki Aza Aoba, Aoba-ku, Sendai, Miyagi 980-0845, Japan

Brief Career:
1991- Kokusai Kogyo Co., LTD.
2014- Project Professor, International Research Institute of Disaster Science, Tohoku University
2018- RTi-cast Inc.

Academic Societies & Scientific Organizations:
• Japan Society of Civil Engineers (JSCE)

Name:
Hiroaki Kobayashi

Affiliation:
Professor, Graduate School of Information Science, Tohoku University

Address:
6-6-01 Aramaki Aza Aoba, Aoba-ku, Sendai, Miyagi 980-8579, Japan

Brief Career:
1988-1991 Research Associate, Tohoku University
1991-1993 Lecturer, Tohoku University
1993-2001 Associate Professor, Tohoku University
1995, 1997-1998, 2001-2002 Visiting Associate Professor, Stanford University
2001- Professor, Tohoku University

Selected Publications:
• R. Egawa, K. Komatsu, S. Momose, Y. Isobe, A. Musa, H. Takizawa, and H. Kobayashi, "Potential of a Modern Vector Supercomputer for Practical Applications – Performance Evaluation of SX-ACE –," J. of Supercomputing, pp. 1-29, doi: 10.1007/s11227-017-1993-y, 2017.
• A. Antonov, A. Frolov, H. Kobayashi, I. Konshin, A. Teplov, V. Voevodin, and V. Voevodin, "Parallel Processing Model for Cholesky Decomposition Algorithm in AlgoWiki Project," Int. J. of Supercomputing Frontiers and Innovations, 2016.
• H. Kobayashi et al. (Eds.), "Sustained Simulation Performance 2015," Springer, ISBN 978-3-319-20340-9, 2015.

Academic Societies & Scientific Organizations:
• Institute of Electrical and Electronics Engineers (IEEE)
• Association of Computing Machinery (ACM)